FILE COPY
NO. 1-W

CASE FILE
COPY

TECHNICAL MEMORANDUMS

NATIONAL ADVISORY COMMITTEE FOR AERONAUTICS

No. 572

IMPACT TESTS ON RUBBER COMPRESSION SPRINGS FOR AIRPLANE LANDING GEARS

By K. Hohenemser

From Zeitschrift für Flugtechnik und Motorluftschiffahrt
March 28, 1930

FILE COPY
To be returned to
the files of the National
Advisory Committee
for Aeronautics
Washington, D. C.

Washington
July, 1930

NATIONAL ADVISORY COMMITTEE FOR AERONAUTICS.

TECHNICAL MEMORANDUM NO. 572.

IMPACT TESTS ON RUBBER COMPRESSION SPRINGS FOR AIRPLANE LANDING GEARS.*

By K. Hohenemser.

It is well known that rubber compression springs are more suitable than rubber tension cords for the absorption of landing shocks, since the former, due to hysteresis, almost completely prevent any bouncing of the airplane. Several types of rubber compression springs made in England have been described and the tension-compression diagrams have been published for several kinds of rubber rings (W. Pleines, "Englische Flugzeugbauverfahren," Flugwoche, 1928, No. 11). It appeared doubtful, however, whether the diagrams obtained from pressure tests could be conclusive for the determination of the safe impact coefficients. The present report gives the results of tests which were made for the purpose of solving this problem. The means for making the tests were kindly placed at our disposal by the Ernst-Ludwigs Gesellschaft.

We shall first explain the operating principle of the rubber compression springs. Figure 1 shows the impression made by a rubber ring when pressed on a glass plate coated with lampblack.

*"Stossversuche an Druckgummifederungen für Flugzeugfahrgestelle." From Zeitschrift für Flugtechnik und Motorluftschiffahrt, March 28, 1930, pp. 133-137.

The structure of the annular surface shows plainly at all points. The structure of both the outer and the inner surface of the ring is portrayed. The distortion therefore occurs in such manner that the material wells forth and presses against the annular surface both inside and out, while the latter adheres perfectly fast and undistorted to the base. When the ring is firmly glued to the compression surfaces, the same pressure diagram is obtained as for the case when it is compressed between glass plates with graphite well rubbed in. It is therefore advisable to glue the rubber rings firmly to the intervening metal disks, since a uniform play is then provided between the inner surface and the guiding tube, without its being necessary to resort to complicated types, such as two-flanged metal disks instead of one, or to the introduction of a special guide ring (Figs. 2 & 3). See the article of Pleines in connection with the above-mentioned devices.

The pressure diagram is greatly affected by the amount of this play. In Figure 4 the pressure is plotted against the per cent of compression for different numbers z of rings. If the inner play is such that the guide tube does not come in contact with the rubber ring even at the maximum compression, the curves for all the z's will coincide with the lowest curve. On the other hand, with the dimensions given in the upper part of Figure 4 and a play of 1.5 mm (0.06 in.), with thirty rings (for example) the frictional force transmitted to the guide

tube for 32% compression is about 70% of the simple elastic counterforce, represented by the lowest curve, and continues to increase with increasing compression. The diagram shows that the rubber ring first comes in contact with the guide tube at about 15% compression. Pressure tests with a ring of the same dimensions, in which was inserted a tightly fitting bolt, showed the remarkable result that the compressive forces corresponding to the same compressions are only slightly greater than for the ring without inside guide tube, although the spreading of the material inward is prevented. The ordinate differences between the curves $z = n$ and the lowest curve of Figure 4 accordingly represent the simple frictional forces on the guide tube.

In itself it is only advantageous when the greatest possible portion of the work to be done by the spring is absorbed by the frictional forces and immediately converted into heat. Still, the frictional force at the maximum compression must not be so great that it can no longer be overcome in the pressure release produced by the elastic force of the rubber, since the spring then remains in the compressed state even after the impact. For the same percentile compressions, the frictional forces on the guide are considerably greater during the loading than during the unloading, as shown by a comparison of the two complete cycles in Figure 5, which obtain for the same ring dimensions as given in Figure 4, the external friction being avoided in plotting the dash curves.

The work, which corresponds to the hysteresis curves, is absorbed by internal friction forces, connected with reaction phenomena. In Figure 5 the loops are plotted for two different maximum loads. The proportional part of the energy destroyed in a load cycle by internal friction forces to the total energy absorbed, increases considerably with increasing maximum compressive force. For the smaller loop in Figure 6 it is 31%; for the larger loop, 41%. All the pressure tests were made with rested material, i.e., the rubber was not loaded for at least two or three hours before the test. If a pressure test was repeated after too short an interval a more strongly bent loading curve was obtained, which has in common with the original curve only the point of maximum load (Fig. 7). In order to show how much smaller the inner friction is in the case of a rubber cable, there is shown in Figure 8 the hysteresis loop for a cable of 9 mm (0.35 in.), which was stretched up to 72% of its original length. Even at this great elongation, the internal energy loss was only 13%.

We designate the forces produced in the deformation of the rubber, when external friction is avoided, as elastic forces, since any separation of the internal friction forces from the real elastic forces is not possible. The impact tests were expected to answer the two following questions.

1. How do the elastic forces of the rubber and their hysteresis vary at deformation velocities such as may occur in landing

impacts, as compared with those of the pressure tests?

2. How do the external friction forces vary?

Figure 9 shows the experimental arrangement. On the round guide rod, which is provided with a length-adjustment nut, slides the guide tube F, which is insured againt rotation by a key engaging in the length nut. To the upper part of the guide tube a number of disk weights G can be applied. The rubber rings R are also on the guide tube. The tube A serves as the anvil on which the plate D strikes. The time-distance diagram of the impact is plotted by means of a recording device S (Fig. 10) on an endless celluloid band which is wound on the drum T, uniformly driven by clockwork. During the fall, the piston K carrying the recording stylus is held by a spring against the stop lever H. After the stylus has passed the top edge of the drum, the stop lever strikes against a stop pin An and releases the piston K, so that the stylus is then pressed against the drum. After the rebound of the rammer, a wooden block is laid on the anvil, so that the stylus does not strike the drum during the second fall. The height of the drum and of the stop pin are both adjustable.

Due to the vibrations of the recording piston, the first part of the diagram was recorded with breaks. The drum had to be so high that the vibrations would be eliminated at the beginning of the impact. This was effected at a falling distance of about 6 cm (2.36 in.). The diagrams were copied from the celluloid band

on to a photographic plate and enlarged 10-15 times by projecting with a projection camera on to millimeter paper, so that the differentiation could be made much more conveniently and accurately than would be possible with the "derivator."

Rubber of rectangular cross section (Continental Quality A.T.G., furnished free by the makers) of various ratios of thickness to outside diameter to inside diameter were tested at falling distances up to 80 cm (31.5 in.) and falling weights up to 20 kg (44 lb.). Figure 11 shows the recorded time-distance diagrams for two rings, which can be deformed without external friction. The intersection points of the O-O line with the diagram indicate the beginning and ending of the impact, these being the time points at which the pressure plate strikes or is raised from the anvil tube. The slight curvature due to gravity is not perceptible, so that the falling parabola appears to be a straight line. In Figure 12, for the same case, the energy absorbed by the rubber during the impact is plotted against the percentile compression and compared with the corresponding curve from the pressure test. OB is the distance traversed by the rammer up to the arrival of the pressure wave. Since the rubber had no initial tension, no energy was given off up to B and the energy required for the compression OB equals the kinetic energy of the rubber. It is small in relation to that of the rammer (or of the airplane), so that we shall disregard it from now on. The dash line is obtained by multiplying the energies or forces

derived from the pressure test at all points by the same coefficient κ, which has the value 2.2 in the case represented. We will call κ the time factor of the elastic forces. It was found that satisfactory accuracy was attained in all cases by using the simple formula

$$P_{eS} = \kappa P_{eD}$$

in which P_{eS} denotes the elastic force of the impact test for any percentile compression and P_{eD} that of the pressure test for the same compression. κ generally depends on the shape of the rings, on the quality of the rubber, on the maximum percentile compression δ_{max} and on the impact time T, i.e., the time up to the maximum compression. It is to be presumed that the value of κ depends chiefly on the ratio δ/T, which represents the mean deformation velocity during the impact. In Figure 13 the values of n from the impact tests are given as a function of δ/T. Although the points are much scattered, it was possible to determine the law from the nature of the plotted curve. No dependence of the form of ring within the variations in the κ values could be established.

We will now consider what mean deformation velocities actually occur in landing impacts. The D.V.L. prescribes, for the "requisite energy absorption" of the landing-gear springs, the value

$$A = c \frac{G}{g} v_l^2 \text{ m kg} \qquad (1)$$

where G denotes the flying weight (full load) in kilograms;

v_l, the landing speed in meters per second; and c, a coefficient which shall have a value of 0.03-0.07 according to the use of the airplane. The value c = 0.07 corresponds, for example, to the case when an airplane strikes the ground at an angle of 1/8.5. We can then obtain an approximate value for the impact time on the assumption of a linear pressure characteristic of the springs (Fig. 14). Let fG denote the initial tension of the springs and eG, the maximum impact force. We then have for the impact time T the expression

$$*T = \left(\frac{\pi}{2} - \text{arc sin } \frac{f}{e}\right)\sqrt{\frac{2\,A}{g\,G\,(e^2 - f^2)}} \qquad (2)$$

---

*Derivation of equation (2):

$$A = f\,G\,s + G\,(e - f)\,\frac{s}{2} \quad \text{(Fig. 14)}$$

$$s = \frac{A}{G}\,\frac{2}{e + f}$$

$$a = \frac{A}{G}\,\frac{2\,f}{e^2 - f^2}$$

Spring constants: $$c = \frac{f\,G}{a} = G^2\,\frac{(e^2 - f^2)}{2\,A}$$

Time for traversing the distance a + s:

$$T' = \frac{1}{4}\,2\pi\,\sqrt{\frac{G}{c\,g}} \quad \text{(1/4 vibration)}$$

Time for traversing the distance s:

$$T = \sqrt{\frac{G}{c\,g}}\left(\frac{\pi}{2} - \text{arc sin } \frac{f}{e}\right)$$

After introducing c:

$$T = \left(\frac{\pi}{2} - \text{arc sin } \frac{f}{e}\right)\sqrt{\frac{2\,A}{g\,G\,(e^2 - f^2)}}$$

As shown by the comparison with the observed impact times, this formula gives too small values for compression rubbers, which, however, even for percentile compressions up to 45%, do not deviate more than 30% from the correct times, although, for such great compressions, the compression curve of the rubber is strongly bent.

The greater the chosen impact multiple e is, the shorter the spring distance (Federweg) s and the softer the spring effect. The landing gear, however, must then be just so much stronger and the fuselage parts must be designed correspondingly. In general, e is not chosen greater than 4. On this assumption and for f = 1, we obtain, at landing speeds of 20-25 m (66-82 ft.) per second, when 1. is inserted in 2., impact times of 0.054 to 0.095 sec. The values occurring in practice fall between the limits of 250 to 500%/s (hatched area in Fig. 13). The time factor of the elastic forces in impacts, corresponding to the "requisite energy absorption" therefore lies somewhere between 1.1 and 1.2.

The share of the internal friction work of the total was not much greater in the impact test than in the pressure test (only 4 to 8%), so that the pressure test yields a good picture of the damping at different maximum compressions (Fig. 6). Further comparative pressure and impact tests were made with rubber rings, which exerted much friction on the interior guide. Even here in both cases there were about the same hysteresis losses, from which it follows that the external friction forces (at least with-

in the given range) are practically independent of the deformation velocity.

We will add a few remarks regarding the best calculation and choice of rubber compression springs. It is first assumed that external friction is avoided. After deciding on definite values for e and f (say e = 4, and f = 1) and distributing the total requisite energy absorption between the wheels and the springs, the assumption of a few other data is necessary, namely, the surface pressure σ_G on the rings at the flying weight G and the maximum percentile compression δ_{max} under the impact force eG.

The smallest possible weight of the springs is obtained by the greatest possible values of σ_G and δ_{max}. The upper limit of σ_G is given by the requirement that the deformation of the rubber under pressure shall not be excessive. Pleines gives a value of 17.6 kg/cm². In the rubber compression springs of the D 18 of the Darmstadt Aero Club, which is calculated for σ_G = 25 kg/cm², very great permanent compressions occurred in the course of a few months, showing that a smaller value should have been adopted for σ_G. For the above limits there are similar standard values for δ_{max} which lie between 40 and 45%. If the inside diameter of the rings with regard to structural considerations is now established, the still lacking characteristic data for the springs, the thickness of the separate rings and the number of the rings can then be definitely determined.

In Figure 15 the surface pressures, as obtained from pressure tests, are plotted against the compressions for a ratio of the inside diameter to the outside diameter of the rings of $d/D = 0.6$ and two different ratios of the height or thickness to the outside diameter h/D. (The percentile compressions refer to the original height zh of the rubber column without intervening metal disks.

The effect of δ_{max} and σ_G on the weight of the rubber column will be shown by an example.* Let $G = 550$ kg, $f = 1$, $e = 4$; the work of the springs $A = 100$ m kg, $d/D = 0.6$, $\kappa = 1.1$. Two rubber columns are used, so that the work for each column is $A_F = 50$ m kg. F = the ring area in cm² and E the energy required for compressing a column of 1 cm² cross section and 100 cm tall betweem $f\,\sigma_G$ and $e\,\sigma_G$.

$$E = \int_{f\sigma_G}^{e\sigma_G} \sigma \, d\delta \text{ kg/cm}^2$$

so that

$$\kappa \, E \, F \, z \, h = A_F \, 100 \quad (h \text{ in cm}).$$

In the accompanying table, the number of rings required, the volume Fzh of the rubber columns and the compression distance (Federweg) s.

*The vertical position of the column is assumed. In practice the oblique position of the spring strut must be considered.

σ_G kg/cm²	δ_{max} %	F cm²	D cm	h/D	h cm	W kg/cm²	Fzh cm³	z	s, cm
15	47	18.4	6.0	0.43	2.5	6.7	680	15	8.5
15	32	18.4	6.0	0.17	1.0	5.4	840	45	8.2
10	47	27.5	7.4	0.43	3.1	5.0	910	11	8.3
10	32	27.5	7.4	0.17	1.25	4.0	1140	33	7.5

It must be remembered that in springs with smaller δ_{max}, not only the weight of the rubber is greater but also more intermediate metal disks are required due to the greater number of rings. It would be desirable for rubber manufacturers to make systematic compression tests with variations of the ratios h : d : D of the rings. It has been found that the elastic forces, and hence the internal friction forces, behave as the squares of the linear dimensions in geometrically similar compression bodies, so that the application of the experimental results to geometrically similar forms is possible.

As a criterion for the suitability of the rubber for airplane landing-gear springs, we can take the "specific energy absorption," i.e., the energy which a piece of rubber of given geometrical shape can absorb per unit of weight at a given percentile compression. The A.T.G. quality of Continental Rubber used by us in all our tests has a specific energy absorption of $A_s = 50$ m kg/kg, if we take as the criterion a test specimen with square compression surfaces, the height of which is equal to half the square side and A_s refers to a compression of 40%. It is also suggested

to the rubber industry to see if a rubber with a higher specific energy absorption can be produced. The specific energy absorption is of prime importance in comparing the different geometrical forms of compression bodies of the same material.

If it is desired to have a portion A_R of the requisite energy absorption absorbed by external friction forces on the rubber rings, the springs must be so calculated in the indicated way that the elastic forces absorb the energy $A_F - A_R$ and the play on the inner guide must be estimated, for which the curves in Figure 4 give approximate reference points. In this case it is expedient to determine the characteristic curve of the springs in advance.

Conclusions

It is first established that the rubber rings adhere firmly to the compression surfaces during the deformation. Suggestions are thus obtained for a constructive simplification of the rubber rings. The hysteresis phenomenon is ascribed to external and internal friction forces. A device for falling tests is then described with which the process of shock absorption with rubber rings was tested. The impact forces agree with the forces of the pressure test to within a factor κ. The time factor κ depends on the mean deformation velocity. For the practical deformation velocities, the impact forces are 1.1 to 1.2 times as large as the forces in the static compression tests. In conclu-

sion, an example is given to show the effect of the assumptions regarding the surface pressure and the maximum percentile compression on the volume and weight of the rubber springs.

Translation by Dwight M. Miner,
National Advisory Committee
for Aeronautics.

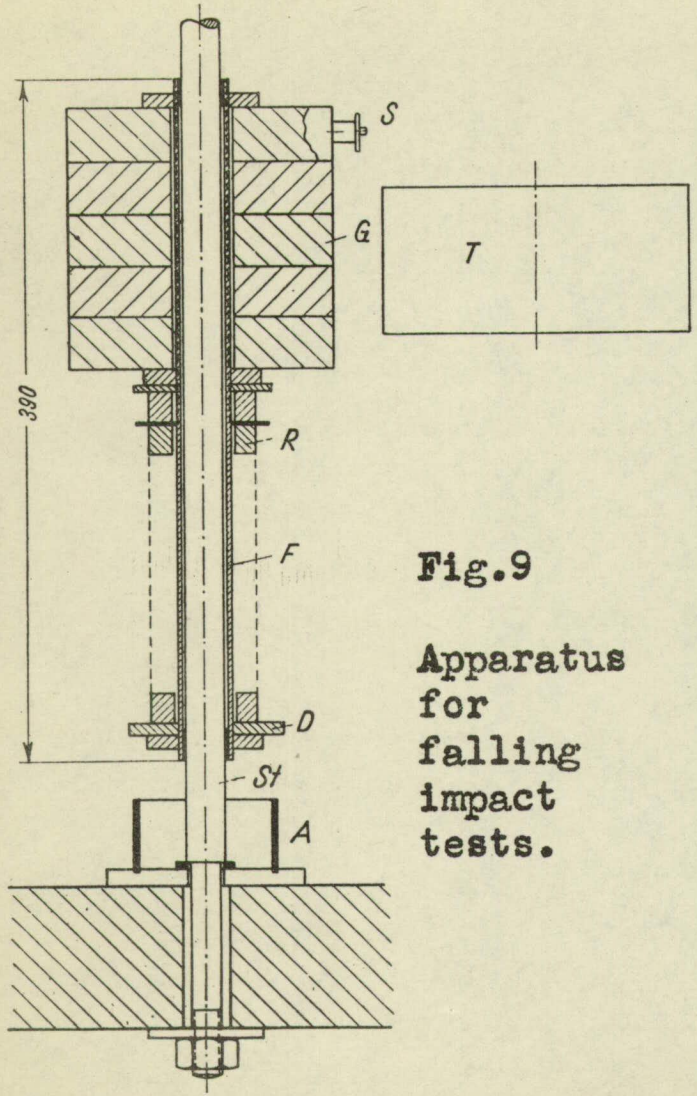

Fig.9

Apparatus for falling impact tests.

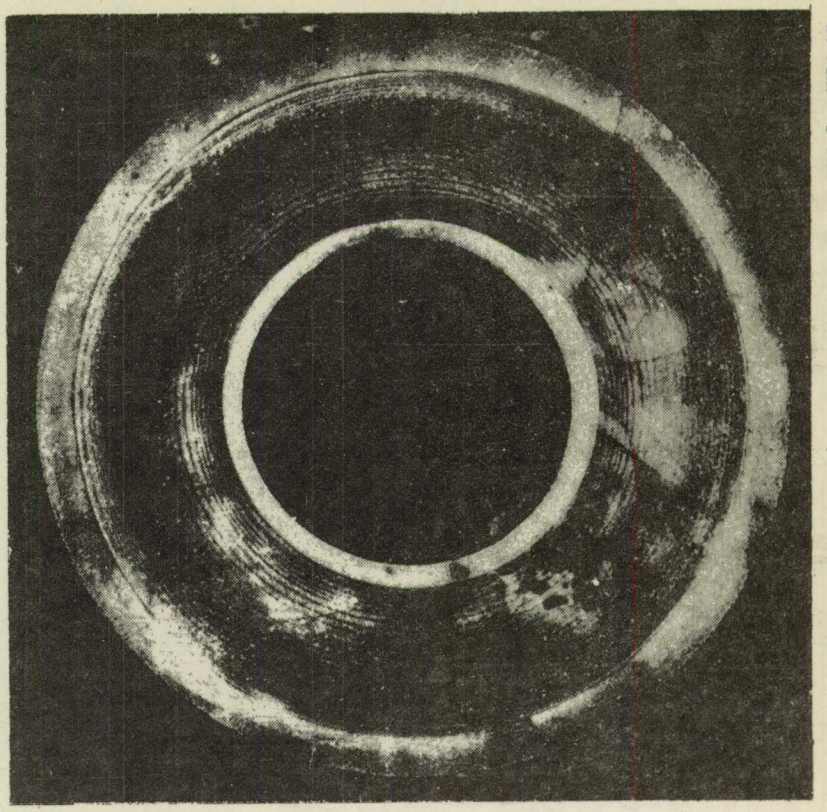

Fig.1

Impression of rubber ring on glass plate, coated with lamp black.

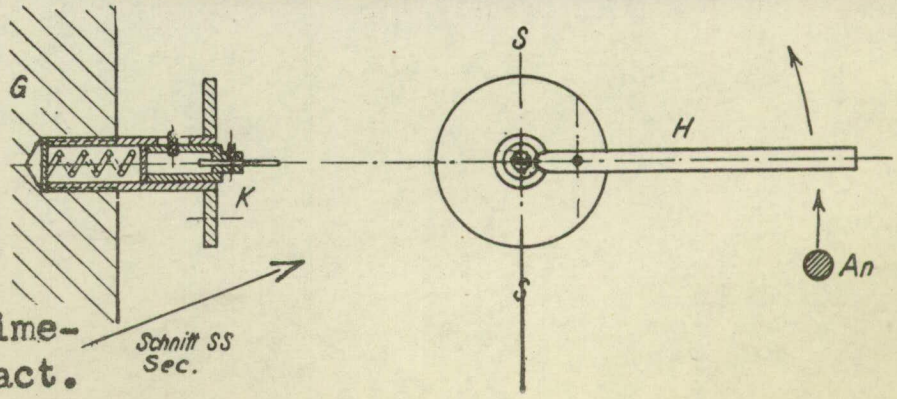

Fig.10 Device for recording the time-distance diagram of an impact.

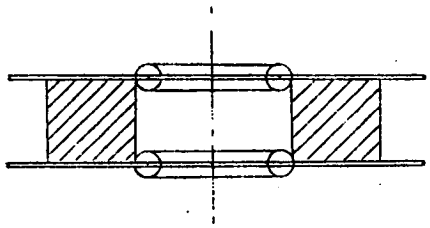

Fig.2 Centering of rubber rings by rolls pressed in the metal disks.

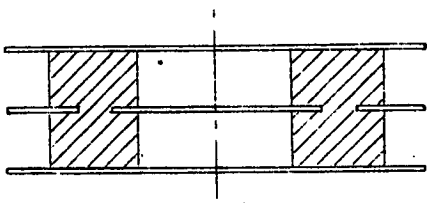

Fig.3 Centering of rubber rings by special inserted metal disks.

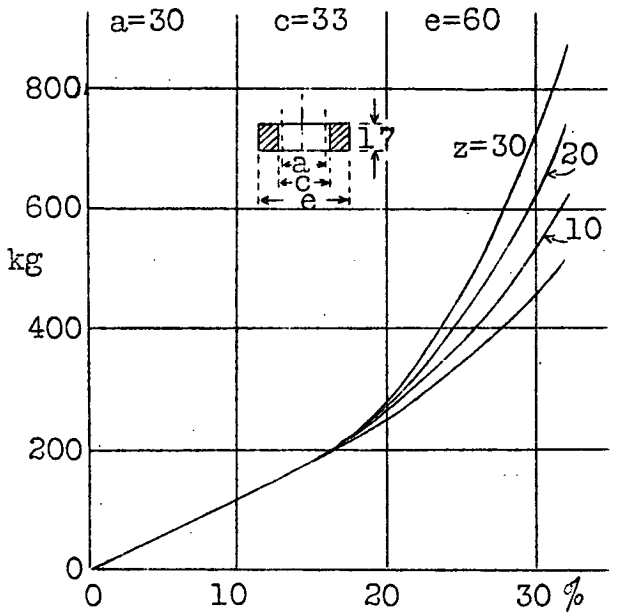

Fig.4 Compressive stress-strain curves for different numbers of rubber rings which rub against the inner guide.

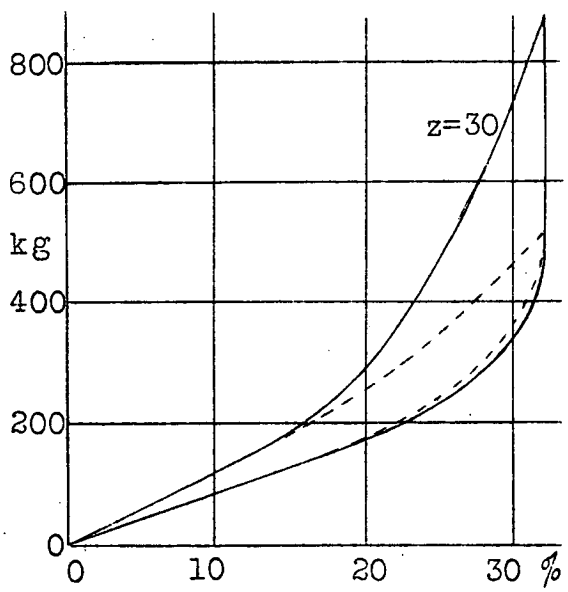

Fig.5 Hysteresis loops with and without external friction.

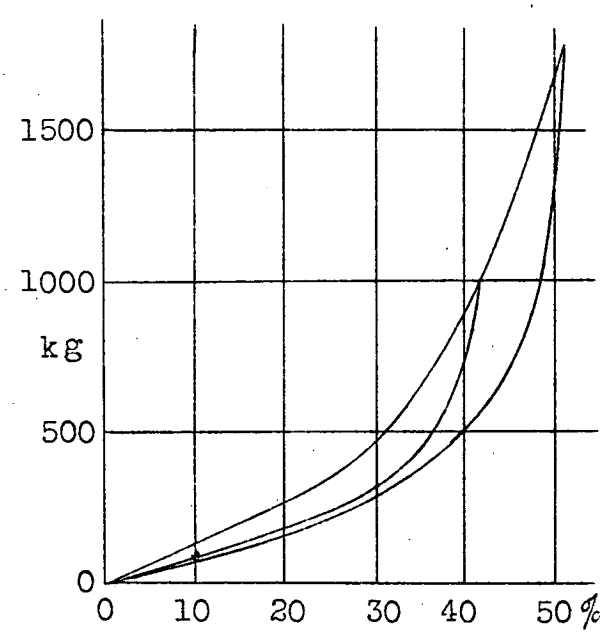

Fig.6 Hysteresis loops without external friction for two different maximum loads.

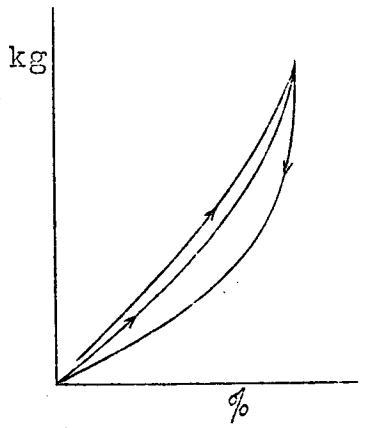

Fig.7 Compressive stress-strain curves for two immediately consecutive loadings.

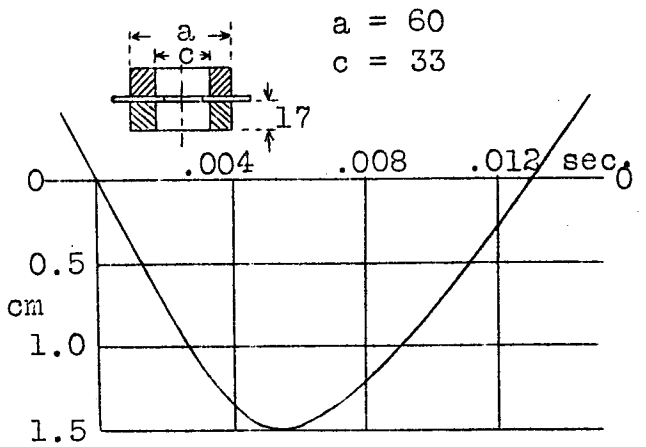

Fig.11 Time-distance diagram for a column of 2 rubber rings.

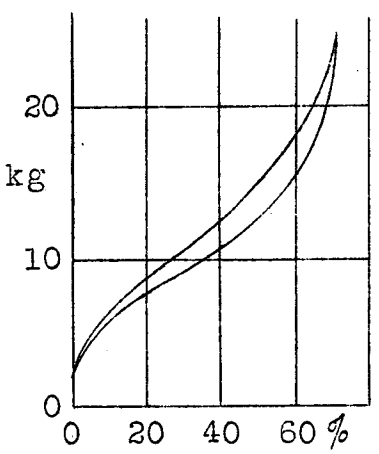

Fig.8 Hysteresis loops for a rubber cable.

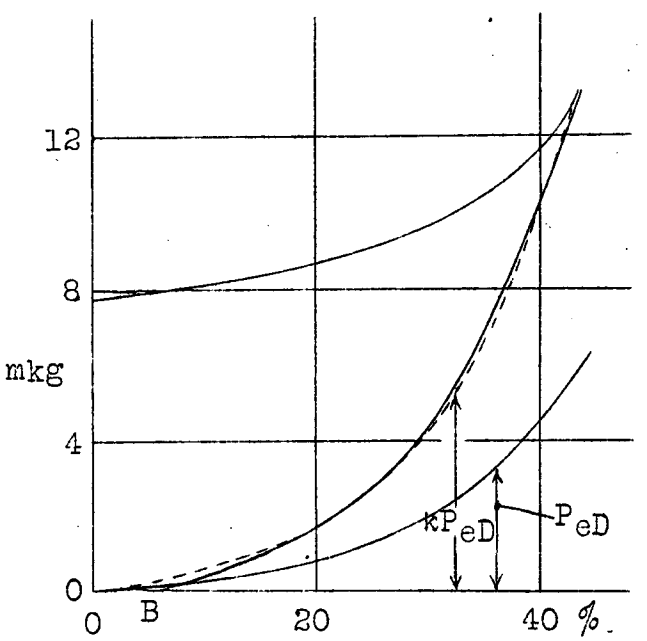

Fig.12 Work diagrams for static and impact loading for the same case as in Fig.11.

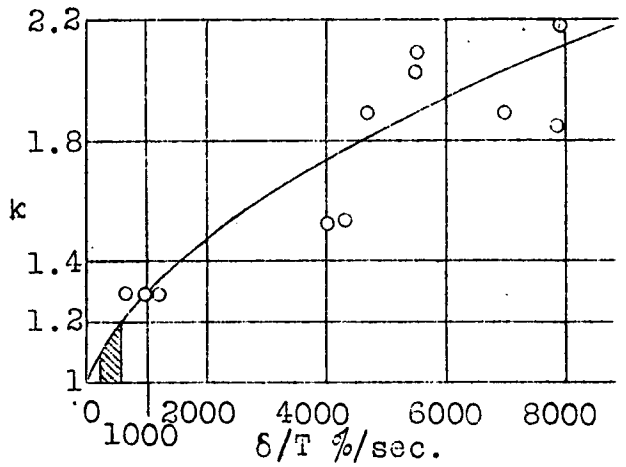

Fig.13 Time factor plotted against deformation velocity.

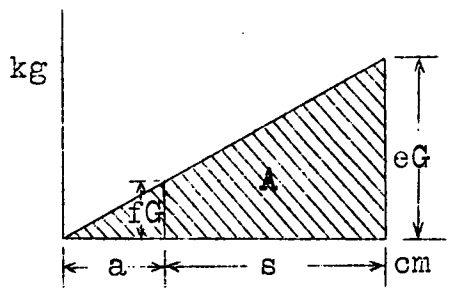

Fig.14 Compressive stress-strain diagram.

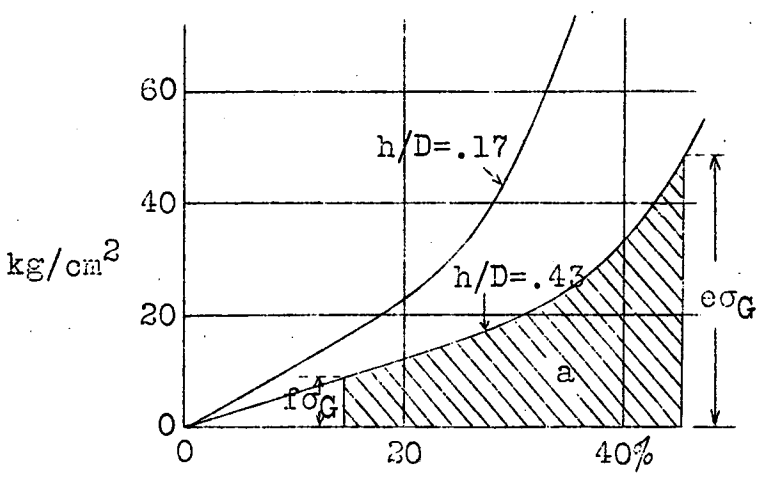

Fig.15 Statically determined tension stress-strain curves for rubber rings with different h/D ratios.